TWO SIMPLE ANALYTICAL MODELS, DIRECT AND INVERSE, FOR SWITCHED RELUCTANCE MOTORS

Liviu E. Somesan*, Emil Padurariu, and Ioan A. Viorel

Electrical Machines and Drives Department, Technical University of Cluj-Napoca, 28 Memorandumului, Cluj-Napoca 400114, Romania

Abstract—This paper presents two simple analytical models of the switched reluctance motor. The first model is constructed on two flux linkage-current characteristics: the aligned position one, calculated via finite element analysis (FEA), and the unaligned position characteristic calculated by using motor geometry data. The second model is based on three flux linkage-current characteristics: the aligned, unaligned and average one, obtained by employing the FEA. In both cases the direct and inverse models are defined. The models consider the core nonlinearity and the influence of the rotor position on the motor behavior. The estimated magnetizing and torque characteristics are compared with that calculated via two dimensions FEA for a switched reluctance motor (SRM) sample and with the test bench obtained ones. The merits and the drawbacks of the models are evinced.

1. INTRODUCTION

The switched reluctance motors (SRM's) advantages, like their simple and robust construction, wide speed range capability, high starting torque and low cost make them attractive alternative to the conventional motors [1, 2].

The SRM's drive performance is strongly dependent on its design and control, which allows for torque ripple reduction [3], or for improving of the torque-speed characteristics. Therefore, it is important to develop an accurate and simple mathematical model of SRM, which facilitates the real-time control of the SRM drive system, or the design process. A key factor for all SRM models are the flux linkage versus current characteristics, which can be calculated analytically, numerically, or by combining the analytic and numeric methods.

Many valuable works dealing with the SRM's mathematical models were published in the past years. Some of them, as [4–7] discussed analytical models based on motor geometry data, while others were dedicated to the SRM models which employ magnetic equivalent circuits [8, 9]. Other models are based on finite element analysis (FEA) [10–25].

In [10], the data obtained via FEA are stored in a lookup-table and any flux linkage-current-position characteristic is calculated by an interpolation procedure. This method is simple but is not very accurate. Recently, magnetic characteristics calculation based on fuzzy logic or artificial neural network (ANN) techniques [11–15], have been reported. The accuracy of these models strongly depends on the amount of given flux linkage-current-position data and on the fuzzy rules or the existing knowledge. Training fuzzy logic and ANN model requires more time and a large amount of initial data. A usual approach is based on the analytical fitting of the previously obtained magnetizing characteristics [16–25].

An accurate analytical model offers advantages in the real-time control of the SRM drive system, or in SRM design process. One, often used, analytical model is obtained by fitting previously given magnetizing characteristics via Fourier series [20–23]. While the model introduced by Chi [22] uses three flux linkage-current characteristics, the one presented in [23] uses five characteristics. Such models are accurate.

In this paper, two mathematical models of SRM are introduced. These models are direct ones, when the flux linkage values are calculated as function of phase currents, and inverse ones, when the current is obtained function of the flux linkage values. A comparison between the estimated magnetizing and torque characteristics and the calculated ones via 2D-FEA, for a sample SRM which was designed, constructed and tested in the laboratory, is given in order to evince the merits and the drawbacks of the models.

The second part of the paper is dedicated to SRM's coupled analytic model which uses geometry data and aligned flux linkage versus current characteristic obtained via 2D-FEA. The direct and inverse models are developed and some calculated results are given for steady-state. This model is an original one, as far as the authors know.

In the third part, an analytical model based on three flux linkage versus current characteristics, obtained via 2D-FEA (unaligned, average and aligned rotor position) is fully developed. The model basics, concerning the two functions which define the rotor position and respectively the core saturation influence, are discussed. The

inverse model is also developed in this case, and some comparisons between the calculated and obtained via 2D-FEA characteristics are given to sustain the accuracy and the consistency of the method. The model initially proposed in [24, 25], is further improved in this paper by adding the procedure to construct the inverse model. Both models are checked on a constructed SRM which is tested in laboratory [26]. The conclusions regarding the accuracy, the simplicity and the usefulness of the discussed models are ending the paper.

2. COUPLED GEOMETRY DATA — FEA MATHEMATIC MODEL

2.1. Model's Basics

The magnetic field analysis via a numerical method, via usually finite element method (FEM), in two or three dimensions, is a compulsory step in SRM's design process. The flux linkage, torque versus current and rotor position characteristics are calculated during the design process employing a 2D-FEA. Once the flux linkage characteristics calculated via 2D-FEA are available, they can be used to develop analytic models. The model presented here is based on motor geometry data and 2D-FEA results obtained for aligned rotor position. The general equation of the flux linkage function of current and rotor position is:

$$\lambda(I_f, \theta) = L_u I_f + (\lambda_a - L_u I_f) \cdot f(\theta) \tag{1}$$

where the unaligned inductance L_u is calculated function of geometry data [4, 5], and I_f is the phase current.

The estimation of the aligned flux linkage characteristics is done by a polynomial ratio [24]:

$$\lambda_a = \frac{I_f}{a \cdot I_f^2 + b \cdot I_f + c} \tag{2}$$

a, b, c coefficients being calculated via a curve fitting procedure applied on the aligned flux linkage characteristic calculated via 2D-FEA.

The position function $f(\theta)$ is [4]:

$$f(\theta) = m(1 - \cos\theta) \tag{3}$$

where the constant m results from the condition:

$$\lambda(I_f, \theta)_{,I_f=I_{\max}, \theta=\theta_a} = \lambda_{a, I_f=I_{\max}} \tag{4}$$

The torque developed by a single phase is:

$$T = \frac{\partial}{\partial \theta} \left(\int_0^{I_f} \lambda \, dI_f \right) \tag{5}$$

The inverse model is given by:

$$I_f(\lambda, \theta) = \frac{a^*\lambda^2 + b^*\lambda}{c^*\lambda + d^*} \cdot \frac{1}{f^*(\theta)} \qquad (6)$$

where a^*, b^*, c^* and d^* are calculated via a curve fitting procedure for the current-flux linkage characteristic in aligned rotor position.

The position function $f^*(\theta)$ is:

$$f^*(\theta) = m \cdot (1 + \cos\theta) \qquad (7)$$

2.2. Results

The proposed analytical models were applied on a SRM in order to check them for viability and accuracy. The main characteristics of a sample 6/4 SRM with 400 W rated power and 2500 rpm are given in Table 1.

**Table 1.** Main geometric dimensions and parameters of sample SRM.

Parameter	Signification	Units	Value
D_{out}	Outer diameter	mm	100
g	Air-gap length	mm	0.4
h_{pS}/h_{pR}	Stator/rotor pole height	mm	17/28
L_{st}	Axial stack length	mm	50
N_t	Number of series turns per pole	-	174
I_n	Phase current	A	2.2
U_f	Phase voltage	V	220

The characteristics calculated based on 2D-FEA results are compared with the ones obtained by employing the discussed model. The flux linkage characteristics for the considered sample are compared in Figure 1. The phase current was incremented by 0.5 A from 0 to 5 A while the rotor position was changed from unaligned position to aligned one. The mechanical rotor position angles are $\alpha = 0°$ (aligned position), $9°$, $15°$, $18°$, $23°$, $27°$, $30°$ and $45°$ (unaligned position).

The torque characteristics of the SRM, Figure 2, are calculated for five phase current values: from 1 A at the bottom to 5 A at the top, the current increment being 1 A.

It is clear that this model, characterized by Equations (1)–(5), is not very accurate but it is simple and has an important advantage since an inverse model can be constructed using the same 2D-FEA calculated characteristics.

The inverse model characteristics are given in Figure 3, while the estimations and functions used for the above presented analytically
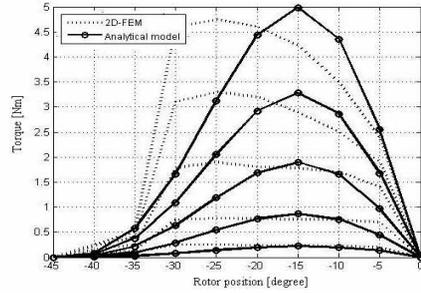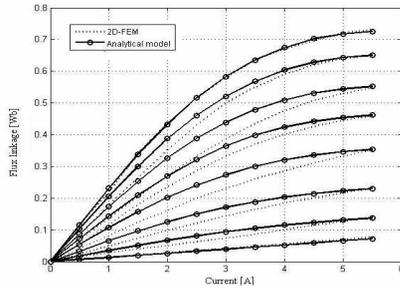
Figure 1. Flux linkage characteristics.

Figure 2. Torque characteristics.
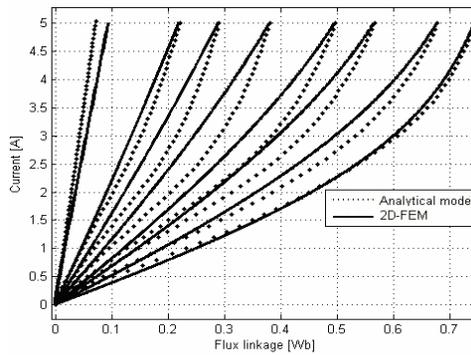
Figure 3. Current versus flux linkage at different rotor positions.

Table 2. Calculated characteristics for direct and inverse models.

	Coupled model	
	Direct	Inverse
Aligned	$\lambda_a\left(I_f\right) = \frac{I_f}{0.1522 \cdot I_f^2 - 0.267 \cdot I_f + 4.463}$	$I_a\left(\lambda\right) = \frac{-51.45 \cdot \lambda^2 + 55.42 \cdot \lambda}{-16.41 \cdot \lambda + 14.77}$
Flux-current	$\lambda(I_f, \theta) = L_u I_f + \left(\lambda_a\left(I_f\right) - L_u I_f\right) \cdot f(\theta)$	$I_f(\lambda, \theta) = \frac{a^* \lambda^2 + b^* \lambda}{c^* \lambda + d^*} \cdot \frac{1}{f^*(\theta)}$
Position function	$f(\theta) = 0.5 \cdot (1 + \cos\theta)$	$f^*(\theta) = \frac{1}{0.5 \cdot (1 + \cos\theta)}$

obtained characteristics in the case of sample SRM are presented in Table 2.

3. DIRECT AND INVERSE MODEL BASED ON MAGNETIC FIELD ANALYSIS RESULTS

3.1. Model's Basics

The model introduced in this part uses only three flux linkage-current characteristics: aligned, average and unaligned, calculated via 2D-FEA. The flux linkage characteristics are given by:

$$\lambda = \lambda_a \frac{l_{0r}}{k_{sr}} \tag{8}$$

The aligned flux linkage characteristic λ_a is estimated via a polynomial function (2). The unsaturated inductance function l_{0r}, which does not depend on current and the saturation function k_{sr} that depends both on current and rotor position, are defined as:

$$l_{0r}(\theta) = a_l + b_l \cos(\theta) \tag{9}$$
$$k_{sr}(I_f, \theta) = a_s(I_f) + b_s(I_f) \cos(\theta) \tag{10}$$

The coefficients a_l, b_l and the polynomial functions $a_s(I_f)$, $b_s(I_f)$ should be obtained via a specific curve fitting procedure, applied step by step.

Three values of unsaturated phase inductance are necessary to obtain the inductance function $l_{0r}(\theta)$: aligned L_{0al}, average L_{0av} and unaligned L_{0un}. The three known values of $l_{0r}(\theta)$ function are:

$$l_{0un} = \frac{L_{0un}}{L_{0al}}, \quad l_{0av} = \frac{L_{0av}}{L_{0al}}, \quad l_{0al} = 1 \tag{11}$$

The $l_{0r}(\theta)$ coefficients, respectively a_1 and b_1, can be calculated through a curve fitting procedure while the $l_{0r}(\theta)$ approximation slightly varies with the number of flux linkage characteristics used.

The saturation function k_{sr} is calculated through a similar procedure that can be applied in two steps.

First, a saturation function depending on the rotor position is calculated at constant current for each considered flux linkage characteristics. If I_f is a given value of the phase current, then the corresponding function k_{sr1} is:

$$k_{sr1}(\theta) = \frac{k_{s1}}{k_{sal1}} = a_{s1} + b_{s1} \cos\theta \tag{12}$$

The coefficients a_{s1} and b_{s1} are obtained through a curve fitting procedure by considering three values of the saturation function k_{sr1} as follows:

$$k_{sr1un} = \frac{k_{s1un}}{k_{s1al}}; \quad k_{sr1av} = \frac{k_{s1av}}{k_{s1al}}; \quad k_{sr1al} = 1; \tag{13}$$

where the suffix notations *un*, *av* and *al* stand for unaligned, average and aligned flux linkage versus current characteristic.

A set of saturation functions for different currents, I_1, I_2, ..., I_f, resulted by using this approach. Finally, the saturation function $k_{sr}(\theta)$ is obtained as:

$$k_{sr}(I_f, \theta) = \frac{k_s}{k_{sal}} = a_s(I_f) + b_s(I_f) \cos \theta \qquad (14)$$

The coefficients $a_s(I_f)$ and $b_s(I_f)$ are polynomial estimations of the existing values a_{s1}, a_{s2}, ... and b_{s1}, b_{s2} ..., respectively.

The way in which the saturation functions are calculated, at different currents, are given in Table 3. The resulting polynomial saturation coefficients $a_s(I_f)$ and $b_s(I_f)$, estimated as explained above, are given in Table 4.
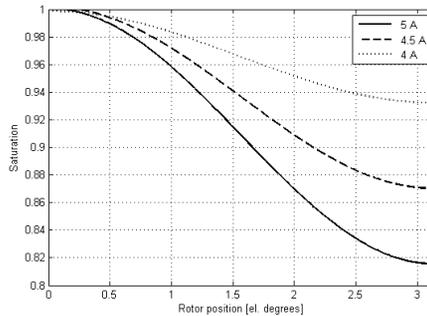
Table 3. Saturation function.

Current	k_{sal}	k_{sav}	k_{sun}	$k_{sr}(\theta)$, $I = ct.$
$I_1 = 5\,\text{A}$	1	0.951	0.791	$0.9152 + 0.1038 \cos(\theta)$
$I_2 = 4.5\,\text{A}$	1	0.966	0.854	$0.9408 + 0.0.07252\cos(\theta)$
$I_3 = 4\,\text{A}$	1	0.981	0.924	$0.9688 + 0.03776 \cos(\theta)$

Table 4. Calculated characteristics for direct and inverse models.

	Model based on FEA-three flux-current characteristics	
	Direct	**Inverse**
Aligned	$\lambda_{al}(I_f) = \frac{I_f}{0.1522 \cdot I_f^2 - 0.267 \cdot I_f + 4.463}$	$I_{al}(\lambda) = \frac{-51.45 \cdot \lambda^2 + 55.42 \cdot \lambda}{-16.41 \cdot \lambda + 14.77}$
Flux-current	$\lambda(I_f, \theta) = \lambda_{al}(I_f) \cdot l_{0r}(\theta)/k_{sr}(I_f, \theta)$	$I(\lambda, \theta) = I_{al}(\lambda) \cdot k_{sr}^*(\lambda, \theta)/l_{0r}^*(\theta)$
Inductance ratio function	$l_{0r}(\theta) = 0.521 + 0.453 \cdot \cos(\theta)$	$l_{0r}^*(\theta) = 0.521 + 0.453 \cdot \cos(\theta)$
Saturation function	$k_{sr}(I_f, \theta) = a_s(I_f) + b_s(I_f) \cdot \cos(\theta)$ $a_s(I_f) = 0.0048 \cdot I_f^2$ $\quad - 0.0968 \cdot I_f + 1.279$ $b_s(I_f) = -0.00969 \cdot I_f^2$ $\quad + 0.1287 \cdot I_f - 0.365$	$k_{sr}^*(\lambda, \theta) = a_s(\lambda) + b_s(\lambda) \cdot \cos(\theta)$ $a_s(\lambda) = 0.0048 \cdot \lambda^2$ $\quad - 0.0968 \cdot \lambda + 1.279$ $b_s(\lambda) = -0.00969 \cdot \lambda^2$ $\quad + 0.1287 \cdot \lambda - 0.365$

The saturation function dependence on rotor position for different current values is presented in Figure 4. As expected, the saturation function has a lower significance at smaller phase current values.

Figure 4. Saturation functions versus rotor position.

The aligned flux linkage characteristic is estimated by a polynomial ratio given by Equation (2), while the torque is calculated via the Equation (5) with a numerical estimation technique that employs the Newton-Cotes method with interpolating Lagrange polynomials of the first degree [27].

The inverse model requires the same three flux linkage-current characteristics, but with an inverse relationship. The inverse equation (with current as the dependent variable) is obtained via a similar procedure as in the case of the direct model.

The flux-current-angle characteristics are given by:

$$I_f(\lambda, \theta) = \frac{I_{al}(\lambda) \cdot k_{sr}^*(\lambda, \theta)}{l_{0r}^*(\theta)} \tag{15}$$

where the functions k_{sr}^* and l_{0r}^* are identical to that defined in Equations (9), respectively (10). The phase current I_{al} in aligned rotor position is:

$$I_{al}(\lambda) = \frac{c \cdot \lambda^2 + d \cdot \lambda}{e \cdot \lambda + f} \tag{16}$$

c, d, e, f being obtained through a curve fitting procedure.

3.2. Results

The resulting characteristics of the sample SRM are given in comparison with that obtained from 2D-FEA, in Figures 5, 6, while the estimations and functions are presented in Table 4. The rotor position and the current values are the same as in the previously given characteristics.

The inverse characteristics: current versus flux linkage and rotor position, are given in Figure 7.
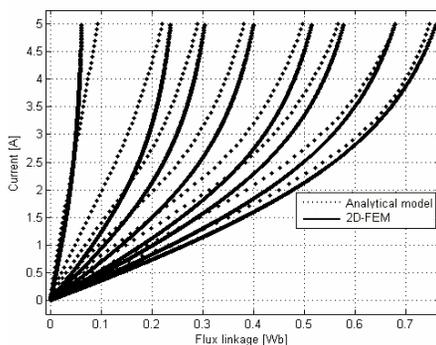
As resulting from the case analyzed, the proposed model is quite accurate and the inverse model is at hand, by using two of direct model functions.
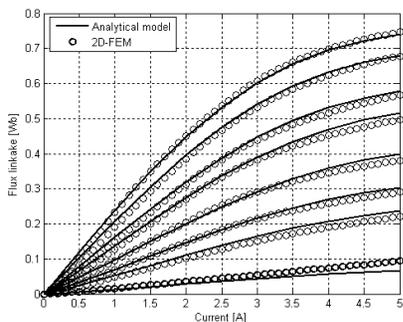
Figure 5. Flux linkage characteristics.
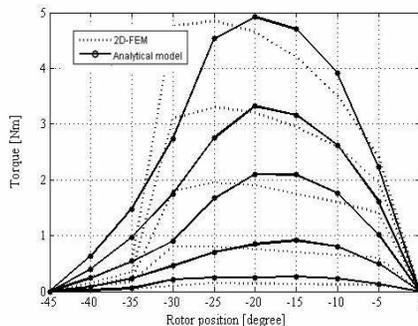
Figure 6. Torque characteristics.

Figure 7. Current versus flux linkage at different rotor positions.

4. CONCLUSIONS

This paper presents two classes of analytical models, one based on geometry data and 2D-FEA calculations while the other one only on flux linkage characteristics calculated via 2D-FEA.

The flux linkage and torque characteristics are calculated using the discussed models for a sample SRM, designed, constructed and tested in the laboratory. The calculated results are compared with the ones obtained for the motor via 2D-FEA, which are compared in the Appendix with the tests.

The comparison between the sample SRM flux linkage-current characteristics obtained via 2D-FEA and by testing the motor on the test bench, Figure A3, evinced the fact that they are in good agreement, as seen in Figure A1 from the Appendix A. Since the 2D-FEA calculated characteristics are smoother than the test

obtained ones, and so are the torque characteristics (A1 and A2), the characteristics calculated via given mathematical models were compared with 2D-FEA characteristics.

A simple model based on geometry data and on flux linkage characteristic, calculated via 2D-FEA in aligned rotor position, is introduced in the paper. The model is obtained in both direct and inverse form.

The model based on three flux linkage characteristics (unaligned, average and aligned rotor position) calculated via 2D-FEA is presented in both direct and inverse form. It is obvious, from the given results, that such a model has an adequate accuracy and covers well the steady state regime of the SRM. A similar model was developed for a linear transverse flux reluctance motor [28] and it can be extended basically on other variable reluctance linear or rotating motors.

The first model is very simple and less accurate than the other one. Its applicability is quite limited to the motor characteristic calculation in the design-sizing stage. The second model is more complicated than the first one, but it is more accurate and it clearly evinces, through the inductance and the saturation functions, the motor nonlinearities. In both cases the inverse model can be constructed quite easy once the direct model is known.

The models presented in the paper are valuable alternative to other similar models, with the same degree of complexity.
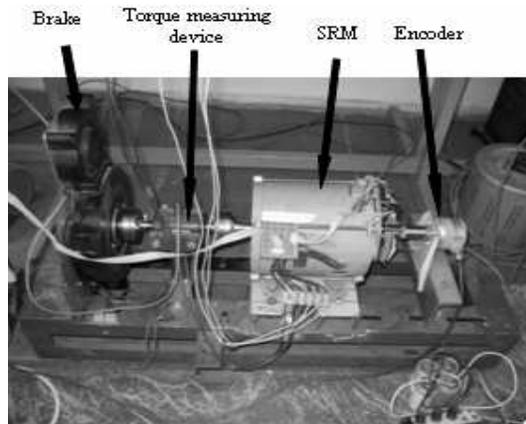
APPENDIX A. CONSTRUCTED AND TESTED SRM
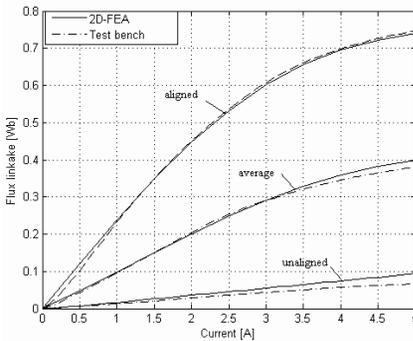
Figure A1. Magnetization curves, obtained on the test bench and calculated via 2D-FEA.
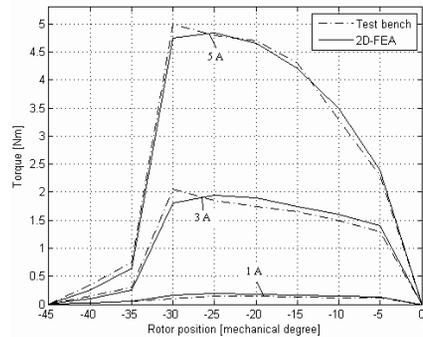
Figure A2. Torque versus rotor position curves, obtained on the test bench and calculated via 2D-FEA.

Figure A3. SRM's test setup.

REFERENCES

1. Krishnan, R., *Switched Reluctance Motors Drives,* CRC Press, 2001.

2. Henneberger, G. and I. A. Viorel, *Variable Reluctance Electrical Machines,* Shaker Verlag, Aachen, Germany, 2001.

3. Stankovic, A. M. G. Tadmor, Z. J. Coric, and I. Agirman, "On torque ripple reduction in current-fed switched reluctance motors," *IEEE Trans. on Ind. Electronics*, Vol. 46, No. 1, 177–183, Feb. 1999.

4. Radun, A. V., "Analytically computing the flux linked by a switched reluctance motor phase when the stator and rotor poles overlap," *IEEE Trans. on Magnetics*, Vol. 36, No. 2, 1996–2003, 2000.

5. Radun, A. V., "Analytical calculation of the switched reluctance motor's unaligned inductance," *IEEE Trans. on Magnetics*, Vol. 35, No. 6, 4473–4481, 1999.

6. Hossain, S. A. and I. Husain, "A geometry based simplified analytical model of switched reluctance machines for real-time controller implementation," *IEEE Trans. on Power Electronics*, Vol. 18, No. 6, 1384–1389, 2003.

7. Khalil, A. and I. Husain, "A fourier series generalized geometry based analytical model of switched reluctance machines," *IEEE Trans. Ind. Appl.*, Vol. 43, No. 3, 673–684, Apr./May 2007.

8. Kokernak, J. M. and D. A. Torrey, "Magnetic circuit model for

mutually coupled switched reluctance machine," *IEEE Trans. on Magnetics*, Vol. 36, No. 2, 500–507, 2000.

9. Preston, M. A. and J. P. Lyons, "A switched reluctance motor model with mutual coupling and multi-phase excitation," *IEEE Trans. on Magnetics*, Vol. 27, No. 6, 5423–5425, 2001.

10. Soares, F. and P. J. Costa, "Simulation of a 6/4 switched reluctance motor based on Matlab/Simulink environment," *IEEE Trans. Aero. Electron.*, Vol. 37, No. 3, 589–609, May 2001.

11. Belfore, L. A. and A. A. Arkadan, "Modeling faulted switched reluctance motors using evolutionary neural networks," *IEEE Trans. on Ind. Electronics*, Vol. 44, No. 2, 226–233, Mar. 1997.

12. Lin, Z. Y. D. S. Reay, and B. W. Williams, "Online modeling for switched reluctance motors using B-Spline neural networks," *IEEE Trans. on Ind. Electronics*, Vol. 54, No. 6, 3317–3321, Nov. 2007.

13. Ding, W. and D. L. Liang, "Modeling of a 6/4 switched reluctance motor using adaptive neural fuzzy inference system," *IEEE Trans. on Magnetics*, Vol. 44, No. 7, 1796–1804, Jul. 2008.

14. Lachman, T., T. R. Mohamad, and C. H. Fong, "Nonlinear modeling of switched reluctance motors using artificial intelligence technique," *IEE Procs. — Elec. Power. Appl.*, Vol. 151, No. 1, 53–60, Jan. 2004.

15. Edrington, C. S., B. Fahimi, and M. Krishnamurthy, "An auto-calibrating inductance model for switched reluctance motor drive," *IEEE Trans. on Ind. Electronics*, Vol. 54, No. 4, 2165–2173, Jul. 2007.

16. Vujicic, V. P., "Modeling of a switched reluctance machine based on the invertible torque function," *IEEE Trans. on Magnetics*, Vol. 44, No. 9, 2186–2194, Sep. 2008.

17. Parreira, B., S. Rafael, A. J. Pires, and P. J. Costa Branco, "Obtaining the magnetic characteristics of an 8/6 switched reluctance machine: From FEM analysis to the experimental tests," *IEEE Trans. on Ind. Electronics*, Vol. 52, No. 6, 1635–1643, Dec. 2005.

18. Zhou, H. J., W. Ding, and Z. M. Yu, "A nonlinear model for the switched reluctance motor," *Proceedings of ICEMS 2005*, Nanjing, China, Oct. 27–29, 2005.

19. Roux, C. and M. M. Morcos, "A simple model for switched reluctance motors," *IEEE Trans. on Energy Conversion*, Vol. 36, No. 3, 400–405, 2005.

20. Andrade, D. A. and R. Krishnan, "Characterization of switched

reluctance machine using Fourier series approach," *Proc. of 36th IEEE Ind. Appl. Annual Meeting*, Vol. 1, 48–54, Sep. 2001.

21. Hue, X. D., K. W. E. Cheng, and S. L. Ho, "Trigonometry-based numerical method to compute nonlinear magnetic characteristics in switched reluctance motors," *IEEE Trans. on Magnetics*, Vol. 43, No. 4, 1845–1848, Apr. 2007.

22. Chi, H.-P., R.-L. Lin, and J.-F. Chen, "Simplified flux-linkage model for switched-reluctance motors," *IEE Procs. — Elec. Power. Appl.*, Vol. 152, No. 3, 577–583, 2005.

23. Xia, C. L., M. Xue, and T. N. Shi, "A new rapid nonlinear simulation method for switched reluctance motors," *IEEE Trans. on Energy Conversion*, Vol. 24, No. 3, 578–586, 2009.

24. Viorel, I. A., L. Strete, and I. F. Soran, "Analytical flux linkage model of switched reluctance motor," *Revue Roum. de Science et Technique, Electrotech. et Energetique*, Vol. 54, No. 2, 139–146, 2009.

25. Somesan, L., E. Padurariu, I.-A. Viorel, C. Martis, and O. Cornea, "Simple analytical models of the switched reluctance motors, case study," *Proceedings of ICEM 2010*, 1–6, Rome, Italy, 2010.

26. Cornea, O., "Control strategies for a SRM drive," Ph.D. Thesis, Politehnica University of Timisoara, 2007 (in Romanian).

27. Chapra, S. C. and R. P. Canale, *Numerical Methods for Engineers,* 3rd Edition, McGraw-Hill Company, 1998.

28. Chang, J. H., D. H. Kang, I.-A. Viorel, and L. Strete, "Transverse flux reluctance linear motor (TFRLM) analytical model based on finite element method (FEM)," *IEEE Trans. on Magnetics*, Vol. 43, No. 4, 1201–1204, 2007.